

## DYNAMICS OF A CAVITATING CASCADE

**Yury A. Semenov**Engineering Science, Osaka University,  
1-3 Machikaneyama, Toyonaka, Osaka, 560-8531, Japan**Abstract**

A method for solving nonlinear problems on unsteady cavity flows within the framework of the model of viscous fluid is proposed. A solution to the nonlinear problem on the unsteady cavity flow past a cascade is presented. Based on linearization of the completely nonlinear solution, a system of equations for calculating the inducer transfer matrix can be obtained.

**1 Introduction**

Cavity flows of low-viscosity fluids are inherently unsteady (Knapp et al. 1970). The flow unsteadiness is due to pulsations of the fluid in the cavity closure region (Michel 1984) where the fluid velocity is far lower than the velocity of the mainstream flow. A high velocity gradient across the wake at a low pressure near the cavity results in fluid discontinuity and in the generation of vortices which form re-entrant flows. The flow pulsations are especially pronounced in flow regimes in which the cavity size is comparable with the size of the body being flown past (partial cavitation). In this case the cavity region is comparable with the region of detached flow in the wake, with the result that the pulsations in the wake have a greater effect on the upstream flow and on the hydrodynamic characteristics of the body being flown past than in the regime of developed cavitation. It should be noted that the regime of partial cavitation is widely encountered because at a small cavity size the time-average hydrodynamic characteristics change only slightly while the occurrence of flow pulsations and unsteady hydrodynamic forces drastically changes the dynamic properties of the flow as a whole and results in far higher dynamic loads on the body and in vibration.

Two approaches are currently at hand in the theoretical study of unsteady cavity flows: one is based on methods of computational hydromechanics, and the other uses numerical-analytical methods for solving inverse boundary-value problems for an ideal incompressible fluid.

The numerical methods for solving cavity flows on the basis of the Navier-Stokes equations have undeniable potentialities (Arndt et al., Kubato et al. 1992, Dieval et al. 1998). However, attempts to simulate the cavity flow medium which is actually discontinuous (because the vapor density is far lower than the liquid density) based on a model of continuous medium are rather tedious and involve, in the present state of the art, an approximate equation of state, which drastically affects the results.

The numerical-analytical methods for solving inverse boundary-value problems assume the formulation of the problem within the limits of an ideal fluid. This brings the cavity closure problem which is responsible for introducing various artificial conditions in the cavity closure region, multiplicity of solutions and differences in the formulation of the partial-cavitation and developed-cavitation flow problems.

The method proposed in this study makes use of the conventional approach for slightly viscous flows which consists in dividing the flow region into a region where the viscous properties of the fluid manifest themselves significantly and an external inviscid flow region which are connected with each other by strong interaction conditions. This approach makes it possible, on the one hand, to allow for the actual properties of the fluid in the cavity wake and, on other hand, to solve the flow in the inviscid region by using well-developed methods for solving cavity flows of an ideal fluid. In addition, the regimes of partial and developed cavitation can be considered within the framework of a single problem. The realization of the proposed method is based on developing a model of unsteady two-phase turbulent detached flow in the cavity wake and mathematical apparatus for solving nonlinear problems on free-boundary unsteady flows based on the theory of functions of complex variable.

Karman was first to use the method of complex potential for solving nonlinear problems on unsteady cavity flows (Karman 1949). Up to now, this approach has not received further development for the lack of a direct method for solving inverse boundary-value problems in nonlinear formulation. A direct method for solving 2D inverse boundary-value problems was proposed in (Semenov 1998). This method makes it possible to find the complex velocity function and the derivative of the complex potential for nonlinear nonstationary problems on cavity flows as easily as the Sokhotski-Plemelj's formula makes it possible to do it for linear problems when

solving Riemann-Hilbert's problem.

The unsteady cavity wake model presented in this paper is based on the flow equations in the boundary-layer theory approximation (Gogish and Stepanov 1979). This assumption is based on the fact that the wake thickness is not great in comparison with the characteristic length, and thus the pressure gradient across the wake can be set equal to zero. The conditions for interaction of the viscous and inviscid flows make it possible to obtain a unique solution to the problem and to study unsteady flows both for an unsteady inflow and for a steady inflow. In the latter case the flow unsteadiness is due to Strouhalian self-oscillations in the wake flow which are typical for most of cavity flows.

For small amplitudes of the parameter perturbations, linearizing the obtained nonlinear solution of the cavity cascade flow makes possible a theoretical calculation of the pressure and flow rate oscillations at the inducer outlet, thus making it possible to calculate the inducer transfer matrix (Brennen and Acosta 1976) over a wide frequency range. It should be noted that the model of the dynamics of a cavitating pump (Pilipenko et al. 1977) which is based on the cavity flow model (Stripling and Acosta 1962) and includes some empirical coefficients makes it possible to calculate the dynamic pump performance up to 50 Hz to an accuracy sufficient for practical purposes. A more rigorous mathematical formulation of the unsteady cavity cascade flow problem within the framework of the linear theory of cavity flows made it possible to extend the frequency range under study and to simulate such types of cavity flow instability as rotating cavitation (Tsujiimoto et al. 1993, Watanabe et al. 1998) and alternate blade cavitation (Horiguchi et al. 1999). A comprehensive overview of the mechanisms of high-frequency oscillations of the cavity flow in an inducer is presented Tsujimoto in the present Symposium.

Further investigations will be aimed at developing an algorithm for solving the nonlinear integro-differential equations derived in this paper with the object of calculating the flow parameter oscillation amplitudes and allowing for nonlinear effects. The analysis of flight test data for different liquid-propellant rockets shows that under POGO oscillations the pressure oscillation amplitudes at the engine inlet are comparable with the average pressure. Because of this, the consensus presently is that under POGO oscillations of most importance are liquid-propellant rocket engine nonlinearities and primarily the nonlinearities involving pump cavitation (Pilipenko 1993, Natanzon 1977).

**2. Nonlinear problem on unsteady cavity flow.**

The two-dimensional unsteady cavity flow of a viscous incompressible fluid past a cascade is considered. By convention, the flow is divided into a viscous turbulent flow region downstream of the cavity and an external inviscid flow region, the cavity *OC* closing on the integral thickness of displacement of the viscous wake *CD*. The condition for strong interaction of the viscous and inviscid flows calls for the velocity at the inviscid flow boundary  $y_\delta$  being equal to the velocity at the outer boundary of the turbulent wake  $\delta$  and for the ordinate of the inviscid flow boundary being equal to the integral thickness of displacement of the viscous wake  $\delta^*$ .

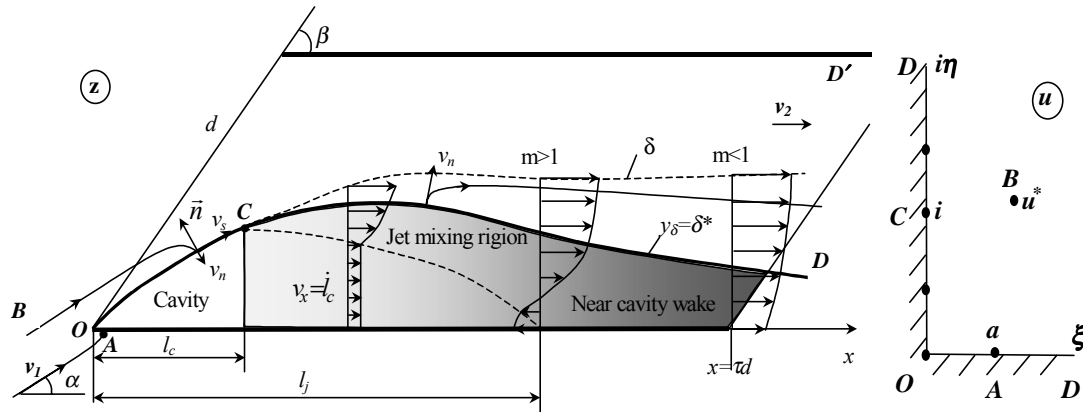


Figure 1: Schematic of unsteady cavity flow past a cascade

**2.1 Solution for the external inviscid flow.** The flow is detached from the edge of the profile at the point *O*. The shape of the cavity closure contour *CD* is not specified beforehand. Along the contour *CD* the velocity modulus function  $v(s,t)$  is specified. Here,  $s$  is the spatial coordinate along the closure contour and  $t$  is time. At the initial instant of time the flow is considered to be steady (or the unsteady flow parameters are specified). What is required is the boundary of the flow region and the flow in this region at subsequent instants of time

provided that the free boundary pressure and the inflow velocity  $v_l$  are given functions of time. The first quadrant is selected as the parameter region (shown in figure 1 is the complex-conjugate flow in the physical plane); the correspondence between the points of the physical plane and those of the parameter plane is shown in figure 1.

The complex velocity for the unsteady flow can be obtained from the corresponding expression for the steady flow by multiplying it by the function

$$f(u) = \exp \left[ -\frac{i}{\pi} \int_0^{\infty} \frac{\partial \ln v}{\partial \eta} \ln \left( \frac{i\eta - u}{i\eta + u} \right) d\eta \right] \quad (1)$$

which is regular in the parameter region and provides the given value of the velocity modulus on the imaginary axis of the parameter region.

Applying Chaplygin's method (Gurevich 1965) for determining the zeros and poles, the final expression for the complex velocity can be written as

$$\frac{dw}{dz} = v_c(t) \left( \frac{u - a(t)}{u + a(t)} \right) \exp \left[ -\frac{i}{\pi} \int_0^{\infty} \frac{\partial \ln v}{\partial \eta} \ln \left( \frac{i\eta - u}{i\eta + u} \right) d\eta \right] \quad (2)$$

Here,  $v(\eta, t)$  is the velocity modulus at the free boundary, i.e. on the cavity contour  $OC$  ( $0 < \eta < i$ ) and the cavity closure contour  $CD$  ( $i < \eta < \infty$ );  $v_c(t)$  is the velocity modulus at the point  $O$ . Setting  $u = \xi$  or  $u = i\eta$  in expression (2), it can be seen that in the parameter region the expression for the complex velocity satisfies the nonpassage condition along the real axis and provides the given value of the velocity modulus along the imaginary axis.

The expression for the derivative of the complex potential can be obtained similarly

$$\frac{dW}{du} = N(t) \frac{u[u^2 - a^2(t)]}{[u^2 - u^{*2}(t)][u^2 - \bar{u}^{*2}(t)]} \exp \left[ \frac{1}{\pi} \int_0^{\infty} \frac{\partial \theta}{\partial \eta} \ln(u^2 + \eta^2) d\eta \right] \quad (3)$$

Here,  $N(t)$  is the scale factor;  $\theta = \arctan(v_n/v_s)$  and  $v_n(\eta, t)$ ,  $v_s(\eta, t)$  are the normal and tangential velocity components at the free boundary.

From expressions (2) and (3) we can obtain

$$\frac{dz}{du} = \frac{N(t)}{v_0(t)} \frac{u[u + a(t)]^2}{[u^2 - u^{*2}(t)][u^2 - \bar{u}^{*2}(t)]} \exp \left[ \frac{i}{\pi} \int_0^{\infty} \frac{\partial \ln v}{\partial \eta} \ln \left( \frac{i\eta - u}{i\eta + u} \right) d\eta + \frac{1}{\pi} \int_0^{\infty} \frac{\partial \theta}{\partial \eta} \ln(u^2 + \eta^2) d\eta \right] \quad (4)$$

Integrating expression (3) in the parameter region allows one to calculate the shape of the free boundary at any time. Time appears in expressions (2) - (4) as a parameter. This reflects the fact that the streamlines are determined by the flow parameters at the current instant of time and do not depend on the history of the fluid flow. The conditions for the inflow velocity and cascade periodicity make it possible to determine the parameters  $a$ ,  $N$ ,  $u^*$ .

$$v_l \exp(-i\alpha_l) = v_0(t) \left( \frac{u^* - a}{u^* + a} \right) \exp \left[ -\frac{i}{\pi} \int_0^{\infty} \frac{\partial \ln v}{\partial \eta} \ln \left( \frac{\eta - u^*}{\eta + u^*} \right) d\eta \right] \quad (5)$$

$$de^{i\beta} = \oint_{u=u^*} \frac{dz}{du} du = 2\pi i \operatorname{res}_{u=u^*} \frac{dz}{du} = \pi i \frac{N}{v_l e^{-i\alpha}} \frac{u^{*2} - a^2}{(u^{*2} - \bar{u}^{*2})} \exp \left[ \frac{1}{\pi} \int_0^{\infty} \frac{\partial \theta}{\partial \eta} \ln(u^{*2} + \eta^2) d\eta \right] \quad (6)$$

The functions  $v(\eta, t)$ ,  $\theta(\eta, t)$  can be found from the dynamic and kinematic boundary conditions at the free surface. On the cavity closure contour  $CD$  the function  $v(\eta, t)$  is determined from the solution of the turbulent flow in the cavity wake.

**Dynamic boundary condition.** The Cauchy-Lagrange integral written for the point  $O$  and for an arbitrary point of the free surface in the physical plane is

$$\frac{\partial \Phi^*}{\partial t} + \frac{p}{\rho} + \frac{v^2}{2} = \frac{\partial \Phi^*}{\partial t} \Big|_{u=0} + \frac{p_v}{\rho} + \frac{v_0^2}{2} = f(t) \quad (7)$$

The potential at the point  $O$  is set equal to zero, therefore  $(\partial \Phi^* / \partial t)_{u=0} = 0$ . Passing to the parametric variable  $\eta = \eta(s, t)$  and the derivative of the potential in the parameter plane, we shall obtain

$$\frac{\partial \Phi}{\partial t}(\eta, t) = \frac{\partial \Phi^*}{\partial t}(s, t) + v \frac{\partial s}{\partial t} \quad (8)$$

Here,  $\Phi^*(s, t) = \Phi[s(\eta, t), t]$ ,  $v$  is the velocity at the point  $s = s(\eta, t)$  and  $(\partial s / \partial t)_{\eta=const}$  is the velocity of motion of the point of the free surface which is due to the time dependence of the parameters appearing in expression (4). The potential  $\Phi(\eta, t)$  at the free boundary can be obtained by integrating expression (3) along the imaginary axis of the parameter region

$$\Phi(\eta, t) = \text{Re}[W(i\eta, t)] = N \int_0^\eta \frac{\eta(\eta^2 + a^2)}{(\eta^2 + u^2)(\eta^2 + \bar{u}^2)} \exp \left[ \frac{1}{\pi} \int_0^\infty \frac{\partial \theta}{\partial \eta'} \ln(\eta'^2 - \eta^2) d\eta' \right] d\eta' \quad (9)$$

In view of expressions (8) and (9), dynamic boundary condition (7) makes it possible to derive an integro-differential equation in the function  $v(\eta, t)$ .

**Kinematic boundary condition.** Let us consider an element  $dz$  of the free boundary in the physical plane. The slope of the boundary at the current instant of time is  $\arg(i dz/d\eta)$ . The variation of the boundary slope at some point is due to the variation of the normal component of the velocity along the boundary, and thus we can write the following equation

$$\frac{\partial}{\partial t} \arg \left( i \frac{dz}{d\eta} \right) = - \frac{\partial v_n}{\partial s} \quad \text{where} \quad ds = |dz| \quad (10)$$

For cavity flows the conditions  $v_n \ll v$  are satisfied, and thus  $\theta$  is small and  $v_n = v_s \tan \theta \approx v\theta$ . Determining  $\arg(i dz/d\eta)$  from expression (4), substituting it into expression (10) and taking into account that  $s = s(\eta, t)$ , it is possible to derive the integro-differential equation in the function  $\theta(\eta, t)$

$$\frac{\partial \theta}{\partial \eta} = -\theta \frac{\partial \ln v}{\partial \eta} - \frac{1}{v^2} \left| \frac{dW}{du} \right|_{u=i\eta} \left( \frac{\partial \theta}{\partial t} + \frac{1}{\pi} \int_0^\infty \frac{1}{v} \left( \frac{\partial^2 v}{\partial t \partial \eta'} - \frac{\partial v}{\partial t} \frac{\partial \ln v}{\partial \eta'} \right) \ln \left| \frac{\eta' - \eta}{\eta' + \eta} \right| d\eta' \right) + \frac{1}{v} \frac{d}{d\eta} \left[ \arg \left( i \frac{dz}{d\eta} \right) \right] \frac{\partial s}{\partial t} \quad (11)$$

Thus the nonlinear problem of solving the unsteady cavity flow is reduced to the system of nonlinear equations (5) – (6) and the system of two integro-differential equations for determining the modulus and normal component of the velocity at the free boundary. To solve the problem, it is necessary to lay down conditions for calculating the velocity modulus at the boundary of interaction of the inviscid flow and the turbulent wake on which the inviscid flow boundary closes.

**2.2. Model of unsteady flow in cavity wake.** When considering the wake flow, two characteristic flow regions can be set aside: a jet region of mixing of the high-velocity flow with the stagnation zone downstream of the cavity and a near cavity wake region. In the jet mixing region the velocity profile is still under formation, and thus the momentum can be ignored. In the near cavity wake the momentum must be allowed for because the velocity profile is completely formed and varies according to the transversal pressure gradient and the inviscid flow boundary.

**Jet mixing region.** In the jet mixing region the velocity projection  $v_x$  is much less than the velocity projection  $v$  at the outer boundary of the mixing region. Thus we can ignore the convective terms in the  $X$ -axis projection of the momentum equation

$$\rho_0 \frac{\partial v_x}{\partial t} = -\frac{\partial p}{\partial x} + \frac{\partial \tau}{\partial y}, \quad \tau = \chi \rho_0 (v - v_x)^2, \quad \frac{\partial \tau}{\partial y} = \frac{\tau}{d} \quad (12)$$

Here,  $\rho_0$  is the density of the two-phase medium averaged across the wake. The tangential stress  $\tau$  is determined by Prandtl's first model of turbulence;  $\chi$  is the turbulence factor and  $d$  is the characteristic dimension of the flow.

The cavity length varies because of the fluid inflow into the cavity and the fluid outflow from the cavity. Thus the averaged velocity across the wake is related to the cavity length variation as

$$v_x = \frac{dl_c}{dt}, \quad l_c = \text{Re} \left[ \int_0^1 \frac{dz}{du} \Big|_{u=i\eta} id\eta \right] \quad (13)$$

**Unsteady near cavity wake.** The flow in the near cavity wake is characterized by the velocity profile formed under the action of the longitudinal pressure gradient and by the shape of the inviscid flow boundary. In the turbulent jet theory (Abramovich 1984) the wake velocity profile can be described by the form parameter  $m$  and the universal function of velocity defect  $f(\bar{y})$

$$\frac{v_x}{v} = 1 - m(x,t)f(\bar{y}) \quad (14)$$

where  $m=(v_\delta v_0)/v_\delta$  is the wake velocity profile form parameter,  $\bar{y} = y/\delta$  is the dimensionless coordinate across the wake,  $v_0, v$  are  $X$ -axis projection of the velocity on the wake axis and the velocity at the outer boundary of the viscous region, respectively, and  $f(\bar{y}) = 2\bar{y}^3 - 3\bar{y}^2 + 1$ . In view of expression (14), the integral displacement thickness  $\delta^*$  and momentum thickness  $\delta^{**}$  are

$$\delta^* = \int_0^\delta \left(1 - \frac{\rho_0 v_x}{\rho v}\right) dy = \delta H^*(m, r) = \delta \left(1 - r + \frac{rm}{2}\right) \quad \delta^{**} = \int_0^\delta \frac{\rho_0 v_x}{\rho v} \left(1 - \frac{v_x}{v}\right) dy = \delta H^{**}(m, r) = \delta \frac{rm}{2} \left(1 - \frac{26}{35}m\right) \quad (15)$$

where  $r = \rho_0 / \rho$  is the relative wake density.

In view of adopted velocity profile (14), the wake flow is described by two functions  $v(x,t)$  and  $m(x,t)$ . To find these functions, we shall use the Karman's integral momentum equation for the unsteady wake obtained by integrating the momentum across the wake allowing for expression (15). Besides, we shall use the equation of flow on the hydrofoil surface ( $y=0$ ) as a second equation

$$\frac{1}{v} \frac{\partial [\delta^* - (1-r)\delta]}{\partial t} + \frac{\delta^*}{v} \frac{\partial \ln v}{\partial t} + \frac{\partial \delta^{**}}{\partial x} + (2\delta^{**} + \delta^*) \frac{\partial \ln v}{\partial x} = 0 \quad (16)$$

$$\rho_0 \frac{\partial v_0}{\partial t} + \rho_0 v_0 \frac{\partial v_0}{\partial x} = \rho \frac{\partial v}{\partial t} + \rho v \frac{\partial v}{\partial x} + \frac{\partial \tau}{\partial y} \Big|_{y=0} \quad (17)$$

The turbulent viscosity is determined in accordance with Prandtl's second model of turbulence

$$\tau = \mu_t \frac{\partial v_x}{\partial y}, \quad \mu_t = \chi \delta \rho_0 (v_{\max} - v_{\min}) \quad (18)$$

where  $\chi$  is the turbulence constant in the near cavity wake and  $v_{\max} = v$  and  $v_{\min} = v_0 = v(1-m)$ .

In view of expressions (15), (16) and (17) can be recast into equations in the velocity at the outer boundary  $v(x,t)$  and  $m(x,t)$ . The density of the vapor-liquid medium  $\rho_0$  ( $r = \rho_0/\rho$ ) in the wake depends on the physical properties of the fluid, flow velocity, gasing, etc. In (Gogish and Stepanov 1982) a relaxation-type equation for time-average cavity flows was proposed. Following this concept, we can write for the unsteady cavity wake

$$\frac{dr}{dt} = \frac{\partial r}{\partial t} + v \frac{\partial r}{\partial x} = v \frac{1-r}{L} \quad (19)$$

where  $L = L(d, Re, We, Q, \dots)$  is the density relaxation scale that depends on the characteristic linear dimension  $d$  and the dimensionless criterial parameters: the number  $Re$ , the number  $We$  and the relative gas content  $Q$ . The pressure in the wake is higher than the vapor pressure. Expression (19) reflects the fact that in the wake the rate of increase of density of an elementary volume of the medium is proportional to the speed and variation of the density in this volume from its equilibrium value.

A computational algorithm for solving the nonlinear problem on unsteady cavity flow was developed for the specific case of the symmetric flow past a plate. The wake model included only the jet mixing region. Shown in figure 2 at the left are dimensionless time dependences of the coefficient of resistance  $C_x$  of the plate, the pressure factor  $C_H = 2(\rho_H - p_c) / (\rho v_\infty^2)$  at the point  $H$  (this point is shown in figure 2 at the right) and the relative cavity length when the cavitation number  $\sigma$  increases as shown in figure 2 at the left.

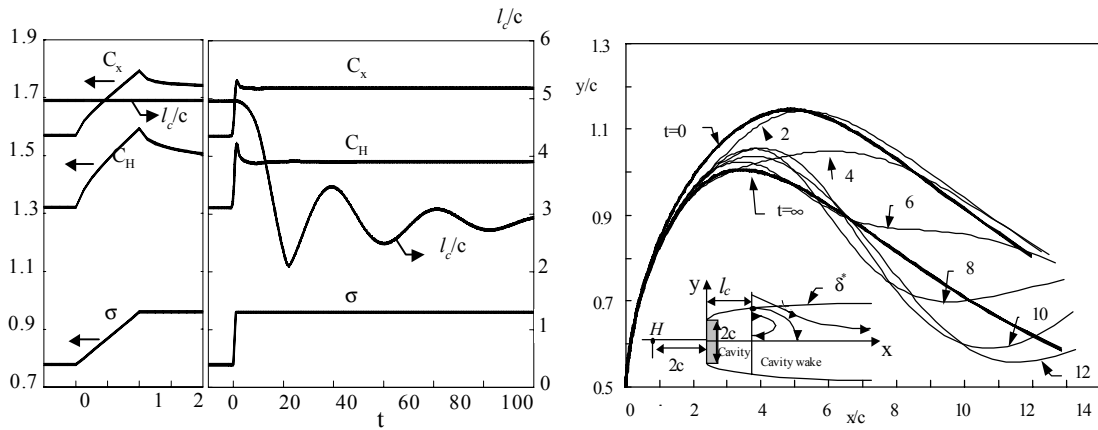


Figure 2: Left: dimensionless time dependences at varying cavitation number. Right: response of the free boundary at varying cavitation number.

The coefficient of resistance of the plate varies nearly synchronously with the cavitation number, and at  $t=1$  it exceeds the value corresponding to the current cavitation number for the steady flow. The cavity length remains constant for  $t < l_c/v_0$  and starts diminishing when the velocity perturbation at the free boundary reaches the cavity closure region and the cavity wake starts moving under the action of an added longitudinal pressure gradient. The Strouhal number determined from the transient that manifests itself as cavity length oscillations is  $Sh=0.05$ . In the calculations, the turbulent viscosity was set higher than it is by a factor of five to make the flow stable. Shown in figure 2 at the right are the contours of the free boundary (cavity boundary and integral thickness of displacement of the viscous wake  $\delta^*$ ) at different instances of time when the cavitation number varies as shown in figure 2 at the left.

### 3 Linearized solutions for small amplitudes of oscillation of the flow parameters

Cavity flows are characterized by the cavity boundary motion velocity being much lower than the fluid velocity, i.e.  $v_n \ll v$ . In addition, for the dynamic properties of the flow to be studied it will suffice to consider the case of small amplitudes of harmonic oscillations of the inflow parameters. In this case the parameters appearing in the solution will also have a small amplitude of oscillation. Thus the parameters appearing in the solution can be represented as

$$a = \bar{a} + \tilde{a}, \quad N = \bar{N} + \tilde{N}, \quad u^* = \bar{u}_s^* + \tilde{u}^*, \quad l_c = \bar{l}_c + \tilde{l}_c, \quad v(\eta, t) = \bar{v}(\eta) + \tilde{v}(\eta, t), \quad \theta(\eta, t) = \bar{\theta}(\eta) + \tilde{\theta}(\eta, t) \quad (20)$$

where barred symbols denote the steady-state values and swung-dashed symbols denote the corresponding perturbations of the parameters. The function  $\bar{\theta}(\eta) \equiv 0$ . In view of expressions (20), expressions (2) – (4), the system of nonlinear equations (5) – (6) and the system of integro-differential equations (7) and (11) can be linearized with respect to the velocity modulus perturbation at the boundary of the inviscid region and the

perturbations of the parameters appearing in the solution. To analyze the stability and dynamic properties of the cavity flow, the perturbations of the parameters appearing in the solution are represented as  $\tilde{a} = \hat{a} \exp(\lambda t)$ ,  $\tilde{N} = \hat{N} \exp(\lambda t)$ ,  $\tilde{u}^* = \hat{u}^* \exp(\lambda t)$ ,  $\tilde{\theta}(\eta, t) = \hat{\theta}(\eta) \exp(\lambda t)$ ,  $\tilde{v}(\eta, t) = \hat{v}(\eta) \exp(\lambda t)$ ,  $\tilde{z}(u, t) = \hat{z}(u) \exp(\lambda t)$ ,  $\tilde{W}(u, t) = \hat{W}(u) \exp(\lambda t)$ , where,  $\lambda = \mu + j\omega$  is the Laplace variable,  $\hat{a}$ ,  $\hat{N}$ ,  $\hat{u}^*$  are the time-complex amplitudes of oscillation of the parameters in the plane of the parametric variable  $u$  and the functions  $\hat{v}(\eta)$ ,  $\hat{\theta}(\eta)$  are the time-complex amplitudes of oscillation of the velocity modulus and of the normal component of the velocity at the free boundary. From expressions (4) - (5) with allowance for expressions (7) and (11), the characteristic equation for determining the Laplace variable can be derived and the natural frequencies of flow oscillation can be determined.

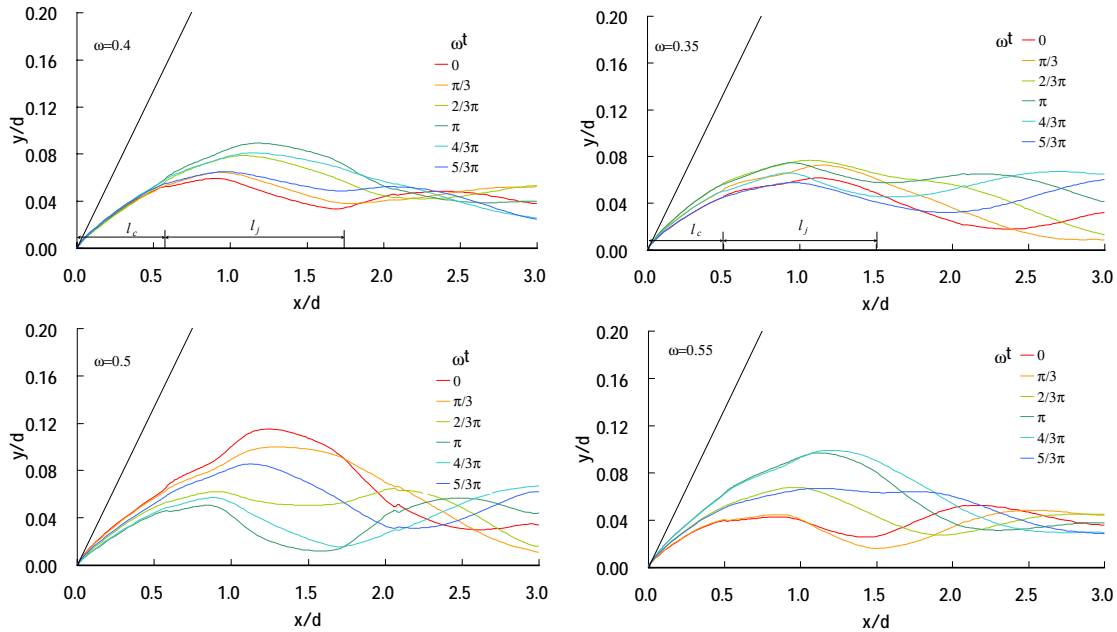


Figure 3: Left: effect of cavitation number oscillations on the shape of the inviscid flow boundary for inlet average cavitation number  $\bar{\sigma} = 0.045$  and amplitude of oscillation  $\tilde{\sigma} = 0.3\bar{\sigma}$ . Right: effect of incidence angle oscillations on the shape of the inviscid flow boundary for inlet average cavitation number  $\bar{\sigma} = 0.065$  and amplitude of oscillation incidence angle  $\tilde{\alpha} = 0.1\bar{\alpha}$ . Both plotted against average incidence angle  $\alpha = 5^\circ$  and inlet cascade angle  $\beta = 15^\circ$

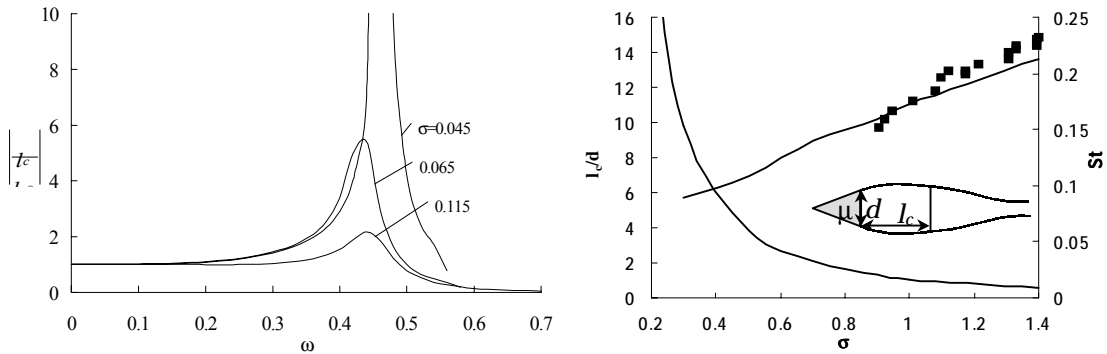


Figure 4: Left: frequency characteristic of the relative cavity length at different values of the cavitation number for inlet cascade angle  $\beta = 15^\circ$ , incidence angle  $\alpha = 5^\circ$  and solidity  $\tau = 3$ . Right: the cavity length and the Strouhal number vs. the cavitation number for the cavity flow past wedge ( $\mu = 60^\circ$ ); squares denote the experimental data (Young and Hall 1966).

Shown in figure 3 are the inviscid flow boundaries under harmonic perturbation of the inflow near the resonance frequency of flow oscillation. At  $\omega t = 0$  the instantaneous value of the cavitation number has a maximum while the incidence angle has a minimum. It can be seen from figure 3 at the left that the variation of the cavity closure contour near the cavity from its mean position changes to opposite when passing the resonance frequency. A similar situation is also observed under harmonic variation of the incidence angle. This is due to the inertial properties of the fluid in the jet mixing region and near cavity wake.

Shown in figure 4 at the left is the amplitude of oscillation of the cavity length normalized to the zero-frequency amplitude versus the oscillation frequency at different values of the cavitation number. The resonance frequency depends only slightly on the cavitation number, and the amplitude increases as the cavity number decreases. The Strouhal number that corresponds to the resonance frequency  $\omega^*$  is  $Sh = (\omega^* d)/(2\pi v_1) \approx 0.072$ . Shown in figure 4 at the right are the time-average cavity length and Strouhal number versus the cavitation number for the cavity flow past a wedge. The calculations were made by the method presented in this paper.

#### 4 Conclusion

An analytical method for solving nonlinear 2D cavity flow problems is presented. The method makes it possible to investigate the dynamics of cavity flows with taken into account viscous wake behind the cavity and determine the unsteady hydrodynamic characteristics, stability and natural frequencies of cavity flows.

#### Acknowledgements

The author would like to express his sincere gratitude to Prof. Y. Tsujimoto who supported the idea of this work, supervised it, made valuable suggestions and reviewed the manuscript. The author is also grateful to Prof. J.M. Michel whose interest in the subject at the previous stage gave impetus to further investigations and to Prof. Y. Yoshida for helpful discussions and suggestions. This study was supported by the JSPS.

#### References

- Abramovich G.N. (1984). *Theory of turbulent jets*. Moscow, (in Russian).
- Arndt, R.E.A., Song, C.C.S., Kjeldsen, M., He., J., and Keller, A. (2000). Instability of Partial Cavitation: A Numerical/Experimental Approach, *Proceedings Twenty Third Symposium on Naval Hydrodynamics*, Val de Reuil, Sept.
- Brennen C., Acosta A., 1976. *Journal of Fluids Eng.*, **89**, 182-191.
- Dieval, L, Arnaud, M. and Marcer, R., 1998. Numerical modeling of unsteady cavitating flows by a VOF method. *Proceedings Third Int. Symposium on Cavitation*, Grenoble, 2: 243-248.
- Gogish L.V. and Stepanov G. Yu. (1979). *Turbulent separated flows*. (in Russian). Moscow, Nauka.
- Gogish L.V. and Stepanov G. Yu. (1982). Turbulent Separated Flows (in Russian) *Izvestia Academy Nauk of USSR. Mekhanika Zhidkostey i Gasa*. Moscow, **2**: 31-47.
- Gurevich M.I. (1965). *Theory of Jets in Ideal Fluids* (in Russian). Moscow, Gos. Izdat Fiz.-Mat. Lit. English trans, New York, Academic.
- Karman T., 1949. Accelerated flow of an incompressible fluid with wake formation". *Ann. Mat. Pura ed Appl. t. XXIX*.
- Knapp, R.T., Daily J.W. and Hammit F.C. (1970). *Cavitation*, New York, McGraw-Hill.
- Kubato, A., Kato, H. and Yamagushi, H. (1992). *J. of Fluid Mech.*, **240**, 59-96.
- Michel, J.M. (1984). *J. of Basic Eng.*, **3**, 319-327.
- Natanzon M.S. (1977). *POGO oscillations of the liquid rockets*. (in Russian), Moscow, Mashinostroenie.
- Otsuka S., Tsujimoto Y., Kamijo K. and Furuya O. (1996). *J. of Fluids Eng.*, **118**, 400 - 408.
- Pilipenko V.V., Zadontsev V. A. and Natanzon M. S. (1977). *Cavitation Oscillations and Dynamics of Hydrosystems* (in Russian), Moscow, Mashinostroenie.
- Pilipenko V.V. (1993). Providing the LPRE - Rocket structure dynamic compability. AIAA Paper N.2422.
- Semenov, Y.A. (1998). Analytical method of solution of 2-D nonlinear problems of free-boundary unsteady flows. *Proceedings 13 U.S. National Congress on Applied Mechanics*, University of Florida, USA.
- Stripling L.B. and Acosta A.J. (1962). *J. of Basic Eng.*, **3**, 29-41.
- Tsujimoto Y. (2001). Simple Rules for Cavitation Instabilities in Turbomachinery. *Proceedings Fourth International Symposium on Cavitation*, Pasadena, California, USA.
- Watanabe S., Tsujimoto Y., Franc J.P. and Michel J.M. (1998). Linear Analyses of cavitation instabilities. *Proceedings Third International Symposium on Cavitation*. Grenoble, France, **1**, 347-352.
- Young J.O. and Hall J.W. (1966). *J. of Basic Engineering*, **1**, 163 - 176.